Ising and Heisenberg models on ferrimagnetic AB_2 chains

2002 J. Phys. A: Math. Gen. 35 9049

(http://iopscience.iop.org/0305-4470/35/43/305)

INSTITUTE OF PHYSICS PUBLISHING JOURNAL OF PHYSICS A: MATHEMATICAL AND GENERAL

J. Phys. A: Math. Gen. **35** (2002) 9049–9061 PII: S0305-4470(02)40019-4

Ising and Heisenberg models on ferrimagnetic AB_2 chains

Carlindo Vitoriano, M D Coutinho-Filho and E P Raposo

Laboratório de Física Teórica e Computacional, Departamento de Física, Universidade Federal de Pernambuco, 50670-901 Recife, PE, Brazil

Received 24 July 2002
Published 15 October 2002
Online at stacks.iop.org/JPhysA/35/9049

Abstract

We study the Ising and Heisenberg models on one-dimensional ferrimagnetic bipartite chains with the special AB_2 unit-cell topology and experimental motivation in inorganic and organic magnetic polymers. The spin-$1/2$ AB_2 Ising case is exactly solved in the presence of an external magnetic field. We also derive asymptotical low- and high-temperature limits of several thermodynamical quantities of the zero-field classical AB_2 Heisenberg model. Further, the quantum spin-$1/2$ AB_2 Heisenberg model in a field is studied using a mean-field approach.

PACS numbers: 75.10.Jm, 75.10.−b, 05.50.+q

1. Introduction

The role of topology in determining many general properties of condensed matter systems has been recognized for a long time. In the context of spin systems, its fundamental influence has been recently explored in the form of special unit-cell configurations and multi-laddered structures. In particular, novel polymeric compounds that are expected to display magnetic properties have been proposed and some of them successfully synthesized [1].

In this work we study the ferrimagnetic bipartite Ising and Heisenberg models on one-dimensional chains [2] with the special AB_2 unit-cell topology, shown in figure 1, and experimental motivation in inorganic [3] and organic [4] magnetic polymers. This type of chain has also been associated with the very unusual magnetic properties observed in the compound $Sr_{0.73}CuO_2$ [5]. Concerning the Hubbard model on these chains, a theorem by Lieb [6] predicts that bipartite AB_2 chains with one electron per site on average (half-filling) and repulsive Coulomb interaction have ground-state spin per unit cell $\hbar/2$, in agreement with numerical techniques, such as Hartree–Fock, exact diagonalization and quantum Monte Carlo [7]. As a consequence of the special unit-cell topology, the very interesting possibility of the existence of unsaturated ferromagnetic or ferrimagnetic long-range ordered ground states has emerged for such systems. In the half-filled strong-coupling limit the AB_2 Hubbard model

0305-4470/02/439049+13$30.00

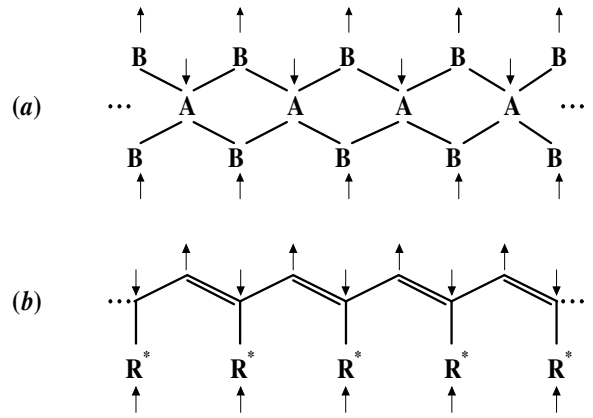

Figure 1. (*a*) Spin chain with AB_2 unit-cell topology displaying the ferrimagnetic ground state in zero magnetic field. In inorganic chains A (B) is a metal (ligand) [3]; $Sr_{0.73}CuO_2$ [5] contains weakly interacting edge-sharing CuO_2 chains. (*b*) ABB' structure exhibiting the ferrimagnetic ground state. In substituted polyacetylenes [4] the lateral radical R^* (B' sites) contains an unpaired electron.

maps [8] onto the quantum AB_2 Heisenberg model with antiferromagnetic (AF) interactions, whose associated quantum nonlinear σ model contains an extra Wess–Zumino term due to the AB_2 topology. Using renormalization-group techniques and scaling analysis, it was shown [8] that this ferrimagnetic system presents low-temperature (low-T) critical properties similar to those of the quantum ferromagnetic AB Heisenberg model, in agreement with the data for the organic ferromagnetic polymer, *p*-NPNN [9]. Further studies on these ferrimagnetic AB_2 chains include rigorous results [10], finite size and conformal invariance [11], density-matrix renormalization group [12], spin-wave and mean-field approximations [13]. It should be noted that there is a close correspondence between the ground-state properties of the AB_2 and mixed-spin chains [11, 12], as evidenced by their spin-wave dispersion relations [13, 14]. Also, the effect of frustration between sites B, not considered here, has been investigated in some detail, including ground-state [15] and thermodynamical [16] properties, as well as magnetic field effects [17]. Besides the various important theoretical aspects put forward in this frustrated case, it is of relevance in the description of several physical properties of the compound $Cu_3Cl_6(H_2O)\cdot 2H_8C_4SO_2$. The effect of the electron–phonon coupling on the formation of spin- and charge-density waves on these systems has also been investigated [18].

In section 2, we exactly solve the spin-1/2 Ising model on an AB_2 chain in the presence of an external magnetic field H. This case is of interest for real systems with very strong uniaxial anisotropy and also to learn about the behaviour of spins on AB_2 chains under freezing of their transversal quantum fluctuations. We study several thermodynamical properties and show that the ferrimagnetic ground state undergoes a first-order phase transition to a paramagnetic state at a critical field H_c. In section 3 we obtain asymptotical low- and high-T limits of several thermodynamical quantities of the classical Heisenberg model on AB_2 chains in zero field. In particular, the leading term of the low-T expansion of the susceptibility is shown to behave as T^{-2}, similar to the quantum [9] and classical [19, 20] AB and quantum AB_2 [8] Heisenberg chains. Finally, section 4 is devoted to the study of the quantum spin-1/2 Heisenberg model on an AB_2 chain in the presence of a field using a mean-field approach. In this case we show that the ferrimagnetic ground state exhibits a continuous phase transition driven by H, such that the unit-cell magnetization increases linearly with H before saturation. Conclusions are presented in section 5.

2. Ising model on AB_2 chains

In the presence of a strong uniaxial anisotropy a magnetic system displays Ising behaviour, a feature which has been widely explored in the context of statistical mechanics and complex systems [21]. In this section, we consider the spin-1/2 Ising model on the bipartite AB_2 chain of N sites ($N/3$ is an integer) shown in figure 1(a). The Hamiltonian of the system is

$$\mathcal{H} = J/\hbar^2 \sum_{\langle i\alpha, j\beta\rangle} \hat{S}_{i\alpha}\hat{S}_{j\beta} - g\mu_B H/\hbar \sum_{i\alpha} \hat{S}_{i\alpha} \tag{1}$$

where $\hat{S}_{i\alpha}$ are Ising spin operators with eigenvalues $\pm\hbar/2$, H denotes the applied magnetic field along the z direction, g is the gyromagnetic factor and μ_B is the Bohr magneton; $J > 0$ is the AF exchange coupling between nearest-neighbour A–B sites, whose locations are denoted by $i\alpha$ and $j\beta$, with $i, j = 1, 2, \ldots, 2N/3$ and $\alpha, \beta = A, B_1, B_2$. In our notation, type A (B) sites are identified by odd (even) i, j indices. No coupling is considered between spins at B sites. Periodic boundary conditions imply that $\hat{S}_{(2N/3)B_1}$ and $\hat{S}_{(2N/3)B_2}$ couple to $\hat{S}_{1A}$. By summing over the Ising variables $S_{i\alpha} = \pm 1$, $\alpha = B_1, B_2$, and requiring the invariance of the partition function after decimation [22], we obtain

$$Z(T, H) = (2f)^{N/3} \sum_{\{S\}} \exp\left[q_1 \sum_{\langle i,j\rangle} S_i S_j + (2q_2 + K_1) \sum_i S_i \right] \tag{2}$$

where $\{S\}$ indicates the sum over all configurations of the remaining $N/3$ spins at sites A (for simplicity we have dropped the labels α, β), $K_1 = \beta g\mu_B H/2$,

$$q_1(T, H) = \frac{1}{2} \ln\left\{ \frac{\cosh[\beta(g\mu_B H - J)/2] \cosh[\beta(g\mu_B H + J)/2]}{\cosh^2(\beta g\mu_B H/2)} \right\} \tag{3}$$

$$q_2(T, H) = \frac{1}{2} \ln\left\{ \frac{\cosh[\beta(g\mu_B H - J)/2]}{\cosh[\beta(g\mu_B H + J)/2]} \right\} \tag{4}$$

and

$$f(T, H) = 2\cosh(\beta g\mu_B H/2)\{\cosh[\beta(g\mu_B H - J)/2] \cosh[\beta(g\mu_B H + J)/2]\}^{1/2} \tag{5}$$

with $\beta = 1/k_B T$. It is thus clear that $Z(N/3) = (2f)^{N/3} Z_0(N/3)$, where $Z_0(N/3)$ is the partition function of the spin-1/2 Ising model on a linear chain of $N/3$ sites, with effective coupling constants J^* between odd sites and effective field H^* given by

$$J^*(T, H) = -\frac{4q_1}{\beta} \qquad H^* = H + \frac{4q_2}{\beta g\mu_B}. \tag{6}$$

Therefore, the Gibbs free energy per site of the ferrimagnetic spin-1/2 AB_2 Ising chain is obtained by inserting equation (6) into the well-known solution of the spin-1/2 linear Ising chain in a field [22]

$$G = -\frac{1}{3\beta} \ln(2f) + \frac{J^*}{12} - \frac{1}{3\beta} \ln\{\cosh(\beta g\mu_B H^*/2) + [\sinh^2(\beta g\mu_B H^*/2) + \exp(\beta J^*)]^{1/2}\}. \tag{7}$$

Before investigating the thermodynamical properties of the system, we find it helpful to look in some detail at the effective coupling constants. In figures 2(a) and (b) we plot J^* and H^* as a function of the dimensionless magnetic field, $g\mu_B H/J$, and dimensionless temperature, $x = k_B T/J$, respectively. As shown in figure 2(a), the effective coupling J^* is negative in general and vanishes for $T = \infty$ in any H (paramagnetic limit). At

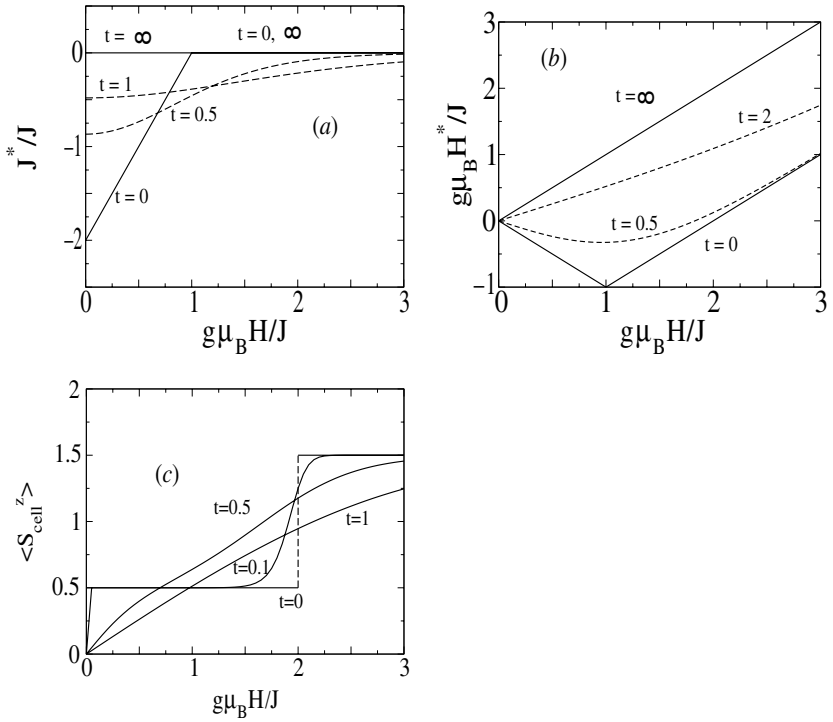

Figure 2. (*a*) Effective coupling constant J^*, (*b*) effective field H^* and (*c*) average spin per unit cell in units of $\hbar$ as a function of the dimensionless magnetic field, $g\mu_B H/J$, and dimensionless temperature, $t = k_B T/J$, for the ferrimagnetic spin-1/2 AB_2 Ising chain.

$T = 0$ and $H = 0$, the result $J^* = -2J$ clearly indicates the presence of a ferrimagnetic structure with spins at the B sites pointing, say, up, and those at the A sites pointing in the opposite direction (see figure 1), thus resulting in a nonzero ground-state spin per unit cell (see figure 2(*c*)). As the field increases at $T = 0$, the magnitude of the effective ferromagnetic coupling between the odd A sites decreases linearly with H and vanishes for $H \geqslant J/g\mu_B$. As one sees from equations (3), (4) and (6), this result reflects the complex interplay between J and H in determining J^*. Conversely, figure 2(*b*) shows that at $T = 0$ the effective field H^* first decreases linearly with H up to $H = J/g\mu_B$. In fact, it is noted in equation (6) that H^* is a result of the applied magnetic field plus a term involving both J and H. Therefore, since H is parallel to the magnetization of the B sites, for $H < J/g\mu_B$ the combined effect with the exchange coupling simulates an effective field pointing parallel to the magnetization of the A sites. For $H = J/g\mu_B$, $J^* = 0$ and $H^* = -H$ is the only remaining effective force to align the magnetization of the A sites. For $H > J/g\mu_B$, H^* increases steadily, changing sign at the critical field $H_c = 2J/g\mu_B$, where a first-order transition to a saturated ferromagnetic state takes place (see figure 2(*c*)). At this transition, both J^* and H^* nullify. At finite temperatures the described effects are less dramatic. For example, J^* is never nullified and only at very low temperatures H^* eventually points antiparallel to H.

Some features of the above discussion clarify the behaviour of the magnetization (magnetic moment per spin) of the system, $M(T, H) = -\partial G/\partial H|_T$, shown in figure 2(*c*). In the $T \to 0$ limit with finite H, we obtain $M(H) = g\mu_B[1 + 2\theta(g\mu_B H - 2J)]/6$, where $\theta(x)$ is the Heaviside function. Note the discontinuity in the ground-state magnetization at the critical

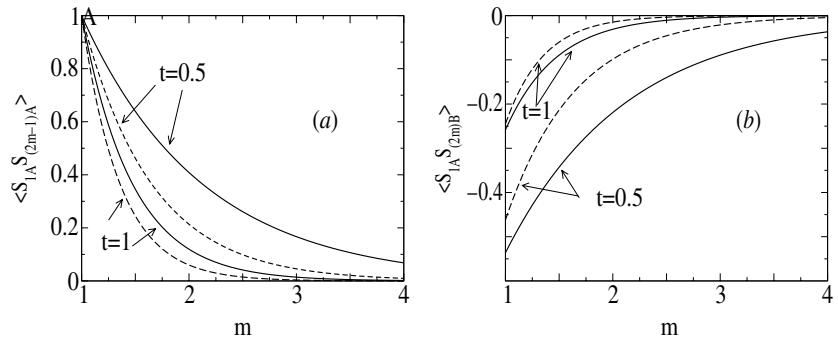

Figure 3. (*a*) Two-spin correlation function as a function of site separation m between A sites of the ferrimagnetic spin-1/2 AB_2 Ising chain (solid curve) and between odd sites of either ferromagnetic or AF spin-1/2 linear Ising chains (dashed curve). (*b*) Two-spin correlation function as a function of site separation m between A and B sites of the ferrimagnetic spin-1/2 AB_2 Ising chain (solid curve) and between even and odd sites of the AF spin-1/2 linear Ising chain (dashed curve). In (*a*) and (*b*) curves are plotted for the dimensionless temperature $t = k_B T/J$.

field $H_c = 2J/g\mu_B$, while for $T > 0$ the zero-field magnetization is null and the step-like behaviour is smoothed out as T increases.

We are also particularly interested in calculating the zero-field thermodynamical limit of the two-spin correlation function, defined by

$$\langle S_{p\gamma} S_{r\delta} \rangle = \lim_{N\to\infty} \frac{1}{Z} \sum_{\{S\}} S_{p\gamma} S_{r\delta} \exp\left(K_2 \sum_{\langle i\alpha, j\beta\rangle} S_{i\alpha} S_{j\beta} \right) \tag{8}$$

where $Z = (2f)^{N/3}[(2\cosh q_1)^{N/3} + (2\sinh q_1)^{N/3}]$ is the zero-field partition function. All kinds of correlation can be expressed in the closed form:

$$\langle S_{p\gamma} S_{r\delta} \rangle = \frac{[-\tanh(\beta J/2)]^u}{[1 + \operatorname{sech}^2(\beta J/2)]^v}. \tag{9}$$

For the case in which both spins are at sites A we choose $p = 1$, $r = 2m - 1$ and $\gamma = \delta = A$, and find $u = 2m-2$ and $v = m-1$ obtained after performing the summation over the even sites in equation (8) followed by additional careful steps. If one considers either a ferromagnetic or an AF Ising chain [20][1] the correlation between parallel spins is given by the numerator of equation (9) with $J \to J/2$, as illustrated in figure 3(*a*), where the AB_2 case is also plotted. For the case in which the spins are at sites A and B we use $p = 1$, $r = 2m$, $\gamma = A$ and $\delta = B_1$ or B_2, so equation (9) applies with $u = 2m - 1$ and $v = m$. Such a result is plotted in figure 3(*b*) and compared with the correlation between antiparallel spins in an AF Ising chain [20]. Finally, we consider the case in which both spins are at sites B (either B_1 or B_2): for $m \geqslant 2$, using $p = 2$, $r = 2m$ and $\gamma = \delta = B$, we obtain $u = 2m - 2$ and $v = m$, whereas for $m = 1$, we get $u = 2$ and $v = 1$, except for the autocorrelation function $\langle S_{2B} S_{2B} \rangle = 1$, as expected.

The above results for the correlation functions can be confirmed through the use of the fluctuation–dissipation theorem:

$$\chi = -\left(\frac{\partial^2 G}{\partial H^2}\right)_{H=0} = \lim_{N\to\infty} \frac{1}{4N} \beta (g\mu_B)^2 \sum_{\langle p\gamma, r\delta\rangle} \langle S_{p\gamma} S_{r\delta} \rangle \tag{10}$$

[1] Note that in the case of the linear Ising model both authors, Thompson and Stanley, consider spin $S = 1$ thus implying an exchange coupling one-quarter of the value used in the present work.

where the factor $1/4$ appears because $S_{p\gamma} = \pm 1$. It reads

$$\chi = \lim_{N\to\infty} \frac{\beta}{4N}(g\mu_B)^2 \sum_{p=1}^{N/3}\sum_{r=1}^{N/3}[\langle S_{(2p-1)A}S_{(2r-1)A}\rangle + 4\langle S_{(2p-1)A}S_{(2r)B}\rangle + 4\langle S_{(2p)B}S_{(2r)B}\rangle]$$
$$= \frac{\beta(g\mu_B)^2}{12[1+\operatorname{sech}^2(\beta J/2)]}\{4\operatorname{sech}^2(\beta J/2) + [1-2\tanh(\beta J/2)]^2[1+\cosh^2(\beta J/2)]\} \tag{11}$$

in which equations (7) and (9) have been used, leading to the same result as above.

Before closing this section one should note that both the H-dependent magnetization and the T-dependent susceptibility are important quantities that characterize the thermodynamical behaviour of the AB_2 Ising chain and may be of interest to help identify the presence of the AB_2 unit-cell topology in magnetic materials under strong uniaxial anisotropy. In fact, deviations from the standard prediction based on pure linear chains, as well as single-ion anisotropy effects, have been extensively studied in real ferrimagnetic compounds [23]. Further, from the results above, as $T \to 0$ and $H = 0$ we obtain the correlation length, $\xi \sim \exp(\beta J)$, and also $\Delta G \equiv G(T) - G(T=0) \sim \xi^{-1}$ and $\chi \sim \xi$, which implies the following relation between the corresponding critical exponents: $\gamma = \nu = 2 - \alpha$. On the other hand, from the behaviour of the correlation function at $T = 0$ and the magnetization at $T = 0$ and $H \to 0$, we find $\eta = 1$ and $\delta = \infty$. The above-described critical behaviour belongs to the same class of universality as a variety of decorated one-dimensional Ising systems [22].

3. Classical Heisenberg model on AB_2 chains

The classical Heisenberg model has been the subject of extensive investigation, particularly in the light of soluble models and rigorous results in statistical physics [2, 20]. Further, the classical Heisenberg chain has been shown to display a rich dynamics in terms of magnons and solitons [24]. In this section we consider the zero-field classical isotropic Heisenberg Hamiltonian on AB_2 chains, defined by

$$\mathcal{H} = J \sum_{\langle i\alpha, j\beta\rangle} \vec{S}_{i\alpha}\cdot\vec{S}_{j\beta} \tag{12}$$

where $J > 0$, $\vec{S}_{i\alpha}$ are classical unit vectors and open boundary conditions are used. The partition function thus reads

$$Z_N = \int\cdots\int\left(\prod_{i\alpha}\frac{\mathrm{d}\Omega_{i\alpha}}{4\pi}\right)\exp\{-\beta J[\vec{S}_1\cdot(\vec{S}_{2B_1}+\vec{S}_{2B_2}) + (\vec{S}_{2B_1}+\vec{S}_{2B_2})\cdot\vec{S}_3 + \cdots + \vec{S}_{(2N/3)-1}\cdot(\vec{S}_{(2N/3)B_1}+\vec{S}_{(2N/3)B_2})]\} \tag{13}$$

in which $\mathrm{d}\Omega_{i\alpha}$ denotes the element of solid angle for the vector $\vec{S}_{i\alpha}$. The free energy per site then follows

$$F(T) = -\frac{1}{\beta}\lim_{N\to\infty}\frac{\ln Z_N}{N} = -\frac{1}{3\beta}\ln\zeta \tag{14}$$

where

$$\zeta = \int\int\frac{\mathrm{d}\Omega_{2B_1}}{4\pi}\frac{\mathrm{d}\Omega_{2B_2}}{4\pi}\exp\left[-\beta J\left(\cos\theta_{2B_1}+\cos\theta_{2B_2}\right)\right]\frac{\sinh\left(\beta J\left|\vec{S}_{2B_1}+\vec{S}_{2B_2}\right|\right)}{\beta J\left|\vec{S}_{2B_1}+\vec{S}_{2B_2}\right|} \tag{15}$$

obtained after integration over Ω_1, with polar axis for $\vec{S}_1$ referred to as $\vec{S}_{2B_1}+\vec{S}_{2B_2}$, whereas the integrations over Ω_{2B_1} and Ω_{2B_2} have $\vec{S}_3$ as the polar axis. Moreover, to derive equation (14)

use was made of the iterating property $Z_N = \zeta Z_{N-3}$, so $Z_N = \zeta^{(N/3)-1}[\sinh(\beta J)/(\beta J)]^2$, in which the last factor is a surface term due to the open boundary condition.

Unlike the one-dimensional AB chain [19, 20], in which case one deals only with single angular integration at each step of the iteration procedure, the double integral in equation (15) presents serious difficulties and thus in the following we derive the asymptotical behaviour of F at high- and low-T. For $\beta J \to 0$, by expanding the integrand of equation (15) up to $\mathcal{O}[(\beta J)^4]$, we obtain

$$F(T) = -\frac{1}{\beta}\left[\frac{2}{9}(\beta J)^2 + \frac{2}{405}(\beta J)^4 + \cdots\right] \qquad \beta J \to 0. \tag{16}$$

The first term of F above is $4/3$ larger than Fisher's result [19], while the second term has a different sign; in both cases the specific heat approaches zero as T^{-2}.

At low-T we note that for the AB_2 ferrimagnetic structure the integrand of equation (15) decreases rapidly for $\left(\theta_{2B_1}, \theta_{2B_2}\right)$ far from (π, π), so we expand it up to second order in the polar angle deviations, $\delta\theta_{2B_1} = \theta_{2B_1} - \pi$ and $\delta\theta_{2B_2} = \theta_{2B_2} - \pi$. The resulting multiple angle integral can thus be evaluated using a saddle-point approach, i.e., by taking the upper limit of polar angle integrations to infinity with negligible error at low-T, thus implying

$$F(T) = \frac{1}{\beta}\ln\beta J + \frac{5}{3\beta}\ln 2 - \frac{4}{3}J - \frac{1}{12\beta^2 J} + \cdots \qquad \beta J \to \infty. \tag{17}$$

The first term of F coincides with that of Fisher [19], while the remaining ones differ in magnitude. It should be noted that this type of low-T expansion presents unrealistic features typical of any classical spin model, particularly concerning the specific heat and entropy behaviour. However, the susceptibility usually displays well-defined low-T behaviour.

In order to calculate the zero-field susceptibility, the thermodynamical limit of the two-spin correlation function should be evaluated:

$$\left\langle S^z_{i\alpha} S^z_{j\beta}\right\rangle = \lim_{N\to\infty} \frac{1}{Z_N} \int \cdots \int \left(\prod_{i\alpha} \frac{\mathrm{d}\Omega_{i\alpha}}{4\pi}\right) S^z_{i\alpha} S^z_{j\beta} \exp\left\{ -\beta J\left[\vec{S}_1 \cdot \left(\vec{S}_{2B_1} + \vec{S}_{2B_2}\right) + \cdots \right.\right.$$
$$\left.\left. + \vec{S}_{(2N/3)-1} \cdot \left(\vec{S}_{(2N/3)B_1} + \vec{S}_{(2N/3)B_2}\right)\right]\right\}. \tag{18}$$

Here we must also consider all distinct correlation functions that have been calculated for the Ising case. We do so by generalizing the approach used to calculate the low- and high-T expansions of the free energy, including the need for the expansion of the integrand up to second order both in polar and azimuthal angle differences. Thus, using equation (11) and omitting the spin-1/2 factor 1/4, the high-T and low-T expansions of the zero-field magnetic susceptibility of the classical ferrimagnetic AB_2 chain read, respectively

$$\chi = \tfrac{1}{3}\beta(g\mu_B)^2\left[1 + \tfrac{8}{9}\beta J + \tfrac{16}{27}(\beta J)^2 + \cdots\right] \qquad \beta J \to 0 \tag{19}$$

$$\chi = \tfrac{2}{9}\beta^2 J(g\mu_B)^2\left[1 - \tfrac{13}{4}(\beta J)^{-1} + \cdots\right] \qquad \beta J \to \infty. \tag{20}$$

The above results should be compared with Fisher's results for the classical ferromagnetic linear Heisenberg chain [19],

$$\chi_F = \tfrac{1}{3}\beta(g\mu_B)^2\left[1 + \tfrac{2}{3}(\beta J) + \tfrac{2}{9}(\beta J)^2 + \cdots\right] \qquad \beta J \to 0 \tag{21}$$

$$\chi_F = \tfrac{2}{3}\beta^2 J(g\mu_B)^2\left[1 - \tfrac{1}{2}(\beta J)^{-1} + \cdots\right] \qquad \beta J \to \infty \tag{22}$$

and that of Takahashi for the quantum ferromagnetic spin-1/2 linear Heisenberg chain at low-T [9]:

$$\chi_T = \frac{2}{3}\beta^2 J(g\mu_B)^2\left[1 - \frac{3\zeta(1/2)}{\sqrt{2\pi}}(\beta J)^{-1/2} + \frac{3\zeta^2(1/2)}{2\pi}(\beta J)^{-1} + \cdots\right] \qquad \beta J \to \infty \tag{23}$$

where $\zeta(1/2)/\sqrt{2\pi} \simeq -0.583$.

From the above equations we note that at high-T the leading term in both Fisher's result and in the AB_2 susceptibility gives the correct paramagnetic limit, also found by Takahashi[2] [9]. At low-T Fisher's and Takahashi's leading terms coincide and are three times larger than that of the AB_2 susceptibility, probably due to a unit-cell effect (AB_2 ferrimagnetic structure) in the low-T and long-wavelength limit. This T^{-2} behaviour was also obtained for the quantum AB_2 Heisenberg chain, but the amplitude of this term could not be fixed by the renormalization-group procedure [8]. It remains to be checked if this amplitude coincides with that calculated for the classical Heisenberg model. Note also that in the quantum case [9], equation (23), there is an extra $(\beta J)^{-1/2}$ term possibly associated with the low-T spin-wave contribution. In fact, this type of contribution dominates the low-T behaviour of the specific heat, $C \propto T^{1/2}$ [8, 9], thus correcting the classical anomalous behaviour [19], as required by the third law of thermodynamics.

4. Quantum Heisenberg model in a field: mean-field approach

The quantum spin-1/2 Heisenberg Hamiltonian on the AB_2 chain is given by

$$\mathcal{H} = J/\hbar^2 \sum_{\langle i\alpha, j\beta\rangle} \hat{S}_{i\alpha} \cdot \hat{S}_{j\beta} - g\mu_B H/\hbar \sum_{i\alpha} \hat{S}^z_{i\alpha} \tag{24}$$

where $J > 0$, the magnetic field H is applied along the z direction and $\hat{S}_{i\alpha}$ denotes the quantum spin operator at the site $i\alpha$, with components defined in terms of Pauli matrices, $\hat{S}^\mu_{i\alpha} = (\hbar/2)\sigma^\mu_{i\alpha}$, $\mu = x, y, z$. Note that, in contrast with the Hamiltonians studied in [15], no coupling between spins at sites B is considered in equation (24). As required in a mean-field approach, the Weiss molecular fields at sites A and B read

$$\langle \hat{S}_A \rangle = -\frac{g\mu_B \hbar}{2J} \vec{H}_B \qquad \langle \hat{S}_B \rangle = -\frac{g\mu_B \hbar}{4J} \vec{H}_A \tag{25}$$

in which $\langle \hat{S}_\alpha \rangle$ represents the quantum thermal mean values of the spin operators and a sum over the nearest-neighbour sites is implied.

First we shall discuss the simplest case in which the molecular fields are assumed to be parallel to the z direction. In this case, the quantum thermal spin values at sites A and B can be used to derive the set of coupled equations for the molecular fields:

$$H_A = -\frac{2J}{g\mu_B} \tanh\left[\frac{\beta g\mu_B (H_B + H)}{2}\right] \qquad H_B = -\frac{J}{g\mu_B} \tanh\left[\frac{\beta g\mu_B (H_A + H)}{2}\right]. \tag{26}$$

Our main goal is to find the ground-state magnetization as a function of H. Therefore, by letting $\beta \to \infty$ in equation (26), we find

$$H_A = -\frac{2J}{g\mu_B} \frac{H_B + H}{|H_B + H|} \qquad H_B = -\frac{J}{g\mu_B} \frac{H_A + H}{|H_A + H|}. \tag{27}$$

Using the conditions, $\lim_{H\to 0^+} \langle \hat{S}^z_A \rangle = -\hbar/2$ and $\lim_{H\to 0^+} \langle \hat{S}^z_B \rangle = \hbar/2$, suitable to describe the AB_2 ferrimagnetic ground state, the solution of equation (27) is found to be

$$H_A = -2J/g\mu_B \qquad H_B = \begin{cases} J/g\mu_B & 0 < H < H_c \\ -J/g\mu_B & H > H_c \end{cases} \tag{28}$$

where $H_c = 2J/g\mu_B$ (see below). From equations (25) and (28), we obtain

$$\langle \hat{S}^z_B \rangle = \hbar/2 \qquad \langle \hat{S}^z_A \rangle = \begin{cases} -\hbar/2 & 0 < H < H_c \\ \hbar/2 & H > H_c \end{cases} \tag{29}$$

[2] Note that Fisher's [19] and Takahashi's [9] exchange couplings and gyromagnetic factors compared to those used in the present work are as follows: $J_F = 2J$, $g_F = 2g$, and $J_T = 4J$, $g_T = 1$ (with $\mu_B = 1$ and $S = 1/2$).

implying the local magnetization per unit cell

$$\langle \hat{S}^z \rangle = 2\langle \hat{S}^z_B \rangle + \langle \hat{S}^z_A \rangle = \begin{cases} \hbar/2 & 0 \leqslant H < H_c \\ 3\hbar/2 & H \geqslant H_c \end{cases} \tag{30}$$

and identifying H_c as the critical field below which the ferrimagnetic ordering is favoured, in agreement with the exact result for the spin-1/2 Ising model on the AB_2 chain (see section 2).

Let us now consider the situation in which the transversal x and y components are also present. In this case, the expectation values at $T = 0$ are given by

$$\langle \hat{S}^z_{A(B)} \rangle = \frac{\hbar}{2} \frac{\left(H^z_{A(B)} + H\right)}{|\vec{H}_{A(B)} + \vec{H}|} \qquad \langle \hat{S}^\mu_{A(B)} \rangle = \frac{\hbar}{2} \frac{H^\mu_{A(B)}}{|\vec{H}_{A(B)} + \vec{H}|} \qquad \mu = x, y. \tag{31}$$

In order to solve the coupled equations (25) and (31), it is convenient to define

$$H_1 = \left[H^2_{Ax} + H^2_{Ay} + (H_{Az} + H)^2\right]^{1/2} \tag{32}$$

$$H_2 = \left[H^2_{Bx} + H^2_{By} + (H_{Bz} + H)^2\right]^{1/2}. \tag{33}$$

It turns out that if $2H_1H_2 \neq H_c^2$, then $H^\mu_A = H^\mu_B = 0$, $\mu = x, y$, and we reobtain the Ising-like solution already discussed. On the other hand, if $2H_1H_2 = H_c^2$ the solution satisfies

$$H_c H^\mu_A = -2H_1 H^\mu_B \qquad \mu = x, y \tag{34}$$

$$H_c\left(H^z_A + H\right) = -2H_1 H^z_B \tag{35}$$

$$H_c\left(H^z_B + H\right) = -H_2 H^z_A. \tag{36}$$

The solution of the equations above is shown to be

$$H^x_A = -H^x_B \qquad H^y_A = -H^y_B \tag{37}$$

$$H^z_A = -\frac{3H_c^2}{8H} - \frac{H}{2} \tag{38}$$

$$H^z_B = \frac{3H_c^2}{8H} - \frac{H}{2} \tag{39}$$

along with the following constraint over H:

$$\frac{H_c}{2} \leqslant H \leqslant \frac{3H_c}{2}. \tag{40}$$

Otherwise the Ising-like solution holds.

It should be noted that, in contrast to H^z_A and H^z_B, the remaining x and y components are undetermined, varying between $H_c/2$ and $3H_c/2$. In spite of this, the magnitude of $\vec{H}_{\alpha\perp} = \hat{x}H^x_\alpha + \hat{y}H^y_\alpha$, $\alpha = A, B$, is precisely determined by the value of H from equations (25) and (41) (see figure 4)

$$|\vec{H}_{A\perp}| = |\vec{H}_{B\perp}| = \frac{\left[\left(9H_c^2 - 4H^2\right)\left(4H^2 - H_c^2\right)\right]^{1/2}}{32H} \tag{41}$$

with fixed angle $\phi = \pi$ between $\vec{H}_{A\perp}$ and $\vec{H}_{B\perp}$.

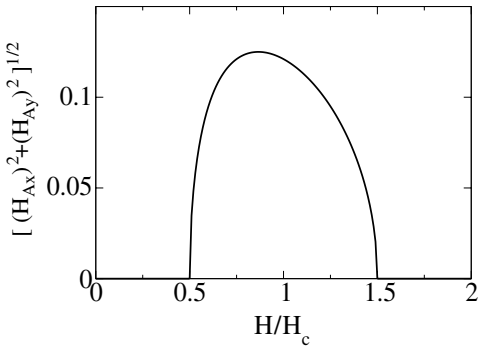

Figure 4. Magnitude of the Weiss molecular field $|\vec{H}_{A\perp}| = (H_{Ax}^2 + H_{Ay}^2)^{1/2}$ as a function of the reduced field, H/H_c, for the quantum ferrimagnetic spin-1/2 AB_2 Heisenberg chain, with $H_c = 2J/g\mu_B$.

We can now proceed to obtain the local z-component of the magnetization on sites A and B. Upon substituting equations (38) and (39) into equation (31), we obtain

$$\langle \hat{S}_A^z \rangle = \begin{cases} -\dfrac{\hbar}{2} & 0 \leqslant H < \dfrac{H_c}{2} \\ -\dfrac{\hbar}{2}\left(\dfrac{3H_c}{4H} - \dfrac{H}{H_c}\right) & \dfrac{H_c}{2} \leqslant H \leqslant \dfrac{3H_c}{2} \\ \dfrac{\hbar}{2} & H > \dfrac{3H_c}{2} \end{cases} \tag{42}$$

and

$$\langle \hat{S}_B^z \rangle = \begin{cases} \dfrac{\hbar}{2} & 0 \leqslant H < \dfrac{H_c}{2} \\ \dfrac{\hbar}{2}\left(\dfrac{3H_c}{8H} + \dfrac{H}{2H_c}\right) & \dfrac{H_c}{2} \leqslant H \leqslant \dfrac{3H_c}{2} \\ \dfrac{\hbar}{2} & H > \dfrac{3H_c}{2} \end{cases} \tag{43}$$

which are plotted in figures 5(a) and 5(b). As seen from these figures, for $0 \leqslant H < H_c/2$ the field aligns the spins in the z direction, with zero average values of the transversal components, while the ferrimagnetic structure is sustained. For $H_c/2 < H < 3H_c/2$ the average spin at sites A continuously rotates seeking a full alignment with the field. This effect is accompanied by a rotation of the spins at sites B, such that for each value of the H the transversal components at sites A and B are cancelled out (see equation (41)). To achieve this cancellation the spins at sites B rotate in the opposite direction up to a maximum polar angle $\theta = 30^\circ$ (from equations (42) and (43)) and then rotate back. The final result is that the unit-cell average spin, $\langle \hat{S}^z \rangle = 2\langle \hat{S}_B^z \rangle + \langle \hat{S}_A^z \rangle$, increases linearly with H for $H_c/2 < H < 3H_c/2$. For $H \geqslant 3H_c/2$ saturation occurs, as shown in figure 5(c):

$$\langle \hat{S}^z \rangle = \begin{cases} \dfrac{\hbar}{2} & 0 \leqslant H < \dfrac{H_c}{2} \\ \dfrac{\hbar H}{H_c} & \dfrac{H_c}{2} \leqslant H \leqslant \dfrac{3H_c}{2} \\ \dfrac{3\hbar}{2} & H > \dfrac{3H_c}{2}. \end{cases} \tag{44}$$

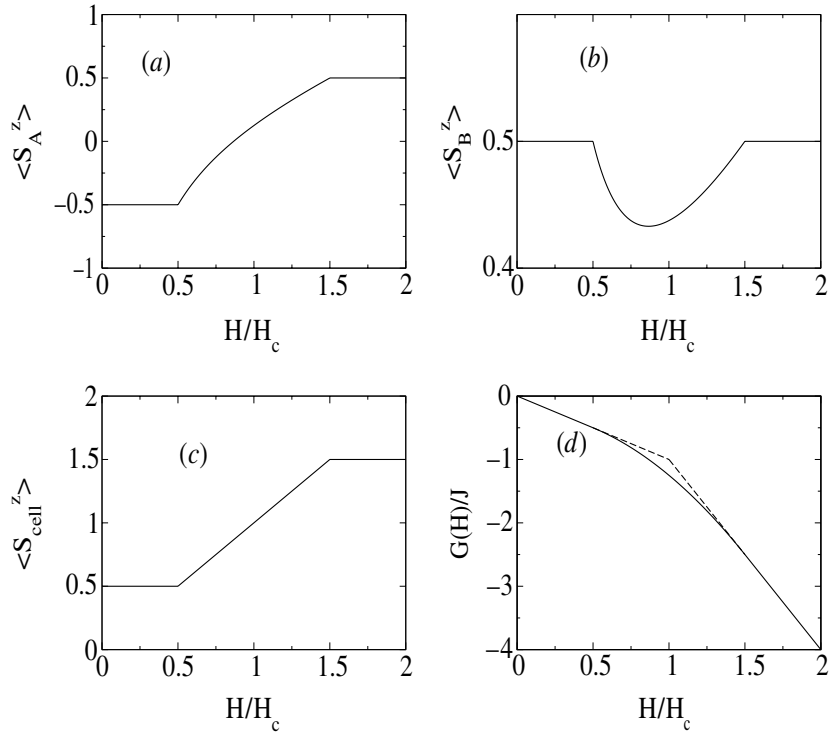

Figure 5. Local magnetization at sites A (a), sites B (b) and per unit cell (c), in units of $\hbar$, as a function of the reduced field, H/H_c, for the quantum ferrimagnetic spin-1/2 AB_2 Heisenberg chain, with $H_c = 2J/g\mu_B$. (d) Field dependence of the Gibbs free energy shows that the continuous solution (solid line) for the magnetization is the stable phase. The Ising-like solution is shown for comparison (dashed line).

It is worth mentioning that a linear increase of the magnetization with H has been observed in an organic magnetic compound exhibiting a canted magnetic structure and attributed to the Dzyaloshinskii–Moriya interaction and an additional weak local anisotropy [25]. Here, the mentioned linear behaviour is due to a combined effect of the exchange force and the special topology of the unit cell. Whether this behaviour is robust under the effect of quantum and thermal fluctuations, particularly near the threshold fields, is an issue for future investigation.

The above features are corroborated by studying the stability of the system through the Gibbs free energy,

$$G(H) = -\int_0^H M(H')\,\mathrm{d}H' \tag{45}$$

along the isotherm $T = 0$. By using the Ising-like solution, equation (30), in equation (45), we obtain

$$G(H) = \begin{cases} -\dfrac{g\mu_B H}{2} & 0 \leqslant H < H_c \\ -\dfrac{3g\mu_B H}{2} + g\mu_B H_c & H \geqslant H_c \end{cases} \tag{46}$$

while the integration of equation (44) using equation (45) yields

$$G(H) = \begin{cases} -\dfrac{g\mu_B H}{2} & 0 \leqslant H < \dfrac{H_c}{2} \\ -\dfrac{g\mu_B H_c}{8} - \dfrac{g\mu_B H^2}{2H_c} & \dfrac{H_c}{2} \leqslant H < \dfrac{3H_c}{2} \\ -\dfrac{3g\mu_B H}{2} + g\mu_B H_c & H > \dfrac{3H_c}{2}. \end{cases} \tag{47}$$

In figure 5(*d*) we compare the solutions given by equations (46) and (47) and conclude that indeed, for $H_c/2 \leqslant H \leqslant 3H_c/2$, the stable magnetization configuration is that with nonzero transversal average spin components.

5. Conclusions

In this work we have studied the Ising and Heisenberg models on one-dimensional bipartite ferrimagnetic chains with the special AB_2 unit-cell topology, shown in figure 1, and experimental motivation in inorganic and organic magnetic polymers. The predicted behaviour for the several reported thermodynamical quantities may appear useful in the identification of the AB_2 structure in real magnetic compounds, as well as for general considerations concerning the presence of magnetic uniaxial anisotropy and the role played by quantum and thermal effects in determining the thermodynamics of this very interesting system. In particular, we mention that while in the Ising version a first-order transition takes place in the presence of a field, in the Heisenberg case a quite exotic continuous spin–flop type transition is predicted, leading to a linear increase of the unit-cell magnetization with field before saturation. Finally, we stress that the thermodynamics of the quantum spin-1/2 Heisenberg model on AB_2 chains still lacks a more complete description. Many features associated with this case are under current investigation using a variety of analytical and numerical techniques.

Acknowledgments

This work was supported by CNPq, Finep, FACEPE and CAPES (Brazilian agencies).

References

[1] Lahti P M (ed) 1999 *Magnetic Properties of Organic Materials* (New York: Dekker)
Miller J S and Epstein A J 1994 *Angew. Chem. Int. Ed. Engl.* **33** 385
[2] For reviews on classical and quantum one-dimensional spin systems, see, e.g., Takahashi M 1999 *One-Dimensional Solvable Models* (Cambridge: Cambridge University Press)
Mattis D C (ed) 1993 *The Many-Body Problem* (Singapore: World Scientific) ch 6
[3] Silvestre J and Hoffmann R 1985 *Inorg. Chem.* **24** 4108
[4] Korshak Y V, Medvedera T V, Ovchinnikov A A and Spector V N 1987 *Nature* **326** 370
Nishide H 1995 *Adv. Mater.* **7** 937
[5] Shengelaya A, Meijer G I, Karpinski J, Zhao G-m, Schwer H, Kopnin E M, Rossel C and Keller H 1998 *Phys. Rev. Lett.* **80** 3626
[6] Lieb E H 1989 *Phys. Rev. Lett.* **62** 1201
Lieb E H 1989 *Phys. Rev. Lett.* **62** 1927
Lieb E H 1993 The Hubbard model: some rigorous results and open problems *Advances in Dynamical Systems and Quantum Physics* (Singapore: World Scientific) p 173
[7] Macêdo A M S, dos Santos M C, Coutinho-Filho M D and Macêdo C A 1995 *Phys. Rev. Lett.* **74** 1851
[8] Raposo E P and Coutinho-Filho M D 1999 *Phys. Rev.* B **59** 14384
Raposo E P and Coutinho-Filho M D 1997 *Phys. Rev. Lett.* **78** 4853
Raposo E P and Coutinho-Filho M D 1995 *Mod. Phys. Lett.* B **9** 817

[9] Takahashi M, Turek P, Nakazawa Y, Tamura M, Nozawa K, Shiomi D, Ishikawa M and Kinoshita M 1991 *Phys. Rev. Lett.* **67** 746
Takahashi M 1987 *Phys. Rev. Lett.* **58** 168
Takahashi M 1986 *Prog. Theor. Phys.* **87** 233
Takahashi M and Yamada M 1985 *J. Phys. Soc. Japan* **54** 2808
[10] Tian G-S and Lin T-H 1996 *Phys. Rev.* B **53** 8196
See also Tian G-S 2001 *Phys. Rev.* B **63** 224413
[11] Alcaraz F C and Malvezzi A L 1997 *J. Phys. A: Math. Gen.* **30** 767
[12] Sierra G, Martín-Delgado M A, White S W, Scalapino D J and Dukelsky J 1999 *Phys. Rev.* B **59** 7973
[13] Vitoriano C, de Brito F B, Raposo E P and Coutinho-Filho M D 2002 *Mol. Cryst. Liq. Cryst.* **374** 185
[14] Ivanov N B 2000 *Phys. Rev.* B **62** 3271
Yamamoto Y, Brehmer S and Mikeska H-J 1998 *Phys. Rev.* B **57** 13610
Pati S K, Ramasesha S and Sen D 1997 *Phys. Rev.* B **55** 8894
[15] Takano K, Kubo K and Sakamoto H 1996 *J. Phys.: Condens. Matter* **8** 6405
Niggemann H, Uimin G and Zittartz J 1997 *J. Phys.: Condens. Matter* **9** 9031
Okamoto K, Tonegawa T, Takahashi Y and Kaburagi M 1999 *J. Phys.: Condens. Matter* **11** 10485
Sano K and Takano K 2000 *J. Phys. Soc. Japan* **69** 2710
[16] Niggemann H, Uimin G and Zittartz J 1998 *J. Phys.: Condens. Matter* **10** 5217
[17] Honecker A and Läuchli A 2001 *Phys. Rev.* B **63** 174407
Tonegawa T, Okamoto K, Hikihara T, Takahashi Y and Kaburagi M 1999 *J. Phys. Chem. Solids* **62** 125
[18] Duan Y-F and Yao K L 2001 *Phys. Rev.* B **63** 13434
[19] Fisher M E 1964 *Am. J. Phys.* **32** 343
See also, Bonner J C and Fisher M E 1964 *Phys. Rev.* **135** A640
[20] Thompson C J 1988 *Classical Equilibrium Statistical Mechanics* (Oxford: Clarendon) ch 3 and 6 and references therein
Stanley H E 1971 *Introduction to Phase Transitions and Critical Phenomena* (New York: Oxford University Press) ch 8 and references therein
[21] Bernardes A T, Florêncio J and Dickman R (ed) 2000 Special issue: Ising centenium colloquium *Braz. J. Phys.* **30** 647
[22] Nelson D N and Fisher M E 1975 *Ann. Phys., NY* **91** 226
Maris H J and Kadanoff L P 1978 *Am. J. Phys.* **46** 652
[23] Fegy K, Luneau D, Belorizky E, Novak M, Tholence J-L, Paulsen C, Ohm T and Rey P 1998 *Inorg. Chem.* **37** 4524
Brandon E J, Rittenberg D K, Arif A M and Miller J S 1998 *Inorg. Chem.* **37** 3376
Wynn C M, Gîrţu M A, Miller J S and Epstein A J 1997 *Phys. Rev.* B **56** 14050
Wynn C M, Gîrţu M A, Miller J S and Epstein A J 1997 *Phys. Rev.* B **56** 315
Wynn C M, Gîrţu M A, Sugira K-I, Brandon E J, Manson J L, Miller J S and Epstein A J 1997 *Synth. Met.* **85** 1695
Wynn C M, Gîrţu M A, Brinckerhoff W B, Sugira K-I, Miller J S and Epstein A J 1997 *Chem. Mater.* **9** 2156
[24] Fogedby H C 1980 *J. Phys. A: Math. Gen.* **13** 1467
Takahashi M 1983 *J. Phys. Soc. Japan* **52** 3592
[25] Palacio F, Antorrena G, Castro M, Burriel R, Rawson J, Smith J N B, Bricklebank N, Novoa J and Ritter C 1997 *Phys. Rev. Lett.* **79** 2336